Preparation of Amphiphilic Mesoporous Carbon-based Solid Acid from Kraft Lignin Activated by Phosphoric Acid and its Catalytic Performance for Hydration of *α*-Pinene

Junkang Xie,[a,b] Qiaoning Han,[a,b] Bo Feng,[a,b] and Zuguang Liu [a,b,]*

An amphiphilic mesoporous carbon-based solid acid (LC_x-SO_3H) with high specific surface area was prepared from kraft lignin that was carbonized using a phosphoric acid treatment. It was found that the specific surface area, pore structure, and amphiphilic nature of the catalyst was effectively controlled through adjusting the phosphoric acid dosage during lignin carbonization. Under optimum preparation conditions, the specific surface area, pore volume, and average pore size of the catalyst were 282.2 m^2/g, 0.26 cm^3/g, and 6.73 nm, respectively. The performance of this solid acid catalyst for the hydration of *α*-pinene was characterized *via* gas chromatography analysis. The conversion of *α*-pinene and the yield of *α*-terpineol during hydration reaction were as high as 95.3% and 55.3%, respectively; these results were greater than the results from other hydration methods with sulfuric acid and commercially available solid acid catalysts (*e.g.*, Amberlyst-15). After five recycles of the carbon-based solid acid without regeneration, conversion of *α*-pinene decreased from 95.3% to 92.6%, and the yield of *α*-terpineol decreased from 55.3% to 47.6%. These observations indicated that the solid acid catalyst derived from kraft lignin carbonization has high potential as a hydration agent for *α*-pinene.

Keywords: Carbon-based solid acid; Lignin; Phosphoric acid; Catalyst; Hydration; α-Pinene

Contact information: a: School of Chemistry and Chemical Engineering, Guangxi University for Nationalities, Nanning, Guangxi, 530008, China; b: Guangxi Key Laboratory of Chemistry and Engineering of Forest Products, Nanning, Guangxi, 530008, China;
** Corresponding author: gxmd311lab@163.com*

INTRODUCTION

The monoterpenic and monocyclic alcohol *α*-terpineol is found in essential oils from nature and is extensively used in the perfume and pharmaceutical industries (Erman 1985). It is unfeasible to separate and purify *α*-terpineol from essential oils at the industrial scale due to its low concentrations in natural plant oils. Currently, *α*-terpineol is synthesized *via* the hydration of *α*-pinene or turpentine using an aqueous mineral acid (such as sulfuric, hydrochloric, or phosphoric acid) or mixed mineral acids as a catalyst (Yuan *et al.* 2016; Prakoso *et al.* 2018). Although the activities of mineral acid catalysts are high, so are the energy requirements needed for catalyst separation, recycling, and the purification of the reaction products (Pakdel *et al.* 2001; Avila *et al.* 2008). Furthermore, equipment corrosion, wastewater treatment, operational hazards, and other factors are issues involved with the *α*-terpineol production processes (Hara *et al.* 2004; Shu *et al.* 2010; Hu *et al.* 2015a). The production costs of *α*-terpineol have increased. In recent years, solid acid catalysts, such as heteropolyacids (Robles-Dutenhefner *et al.* 2001), ion exchange resins (Yang *et al.* 2011), and solid superacids (Liu *et al.* 2013), have been examined for the production of α-terpineol. Such acid catalysts are easily recycled and have lower environmental impacts (Vital *et al.* 2000). Among all of the types of solid acid catalysts, the carbon-based ones are considered promising candidates due to their low cost, wide range of textural properties, and relatively high density of sulfonic acid groups (Okuhara 2002). Moreover, more bioresources are being used as starting materials for their easy preparation and regeneration, and their excellent mechanical and thermal stabilities effectively increase their potential for practical application in acid catalytic reactions over other solid acid catalysts (Geng *et al.* 2011; Malins *et al.* 2015). Carbon-based solid acids can be classified as either supported or functionalized catalysts.

Functionalized carbon-based solid acids can be prepared by direct sulfonation or indirect sulfonation *via* alkylation or arylation (Malins *et al.* 2015). Carbon-based solid acids can be produced by the direct sulfonation of cellulose, glucose, glycerol, starch, or polymers (Budarin *et al.* 2006; Fukuhara *et al.* 2011; Song *et al.* 2012; Zhao *et al.* 2016; Li and Zeng 2017; Zhang *et al.* 2017; Li *et al.* 2018). In recent years, biomass resources, such as corn cob, rice straw, bagasse, peanut husk, *etc*., have been used as the raw substrate for the preparation of carbon-based solid acid catalysts (Bedia *et al.* 2010; Ezebor *et al.* 2014; Wang *et al.* 2014; Zeng *et al.* 2014; Haziratul Mardhiah *et al.* 2017; Wang *et al.* 2017; Qi *et al.* 2018). To increase the specific surface area of the solid catalysts, activators often have been used during the preparations of the catalysts. Although catalysts with large specific surface area can be obtained through this method, the porosity of such catalysts is predominated by micropores, and the amphiphilicity of the surface of the catalysts was not investigated (Tang and Niu 2019). Such solid acid catalysts might not be suited for hydration reactions of alkenes, although they may have high catalytic activities for other types of reactions.

Lignin is the second most abundant organic polymer found in nature after cellulose (Liu *et al.* 2016). Technical lignins are produced at levels of around 70 million tons per year and are a renewable industrial byproduct from the chemical pulping of wood. However, this byproduct has not been used efficiently (Gosselink *et al.* 2004; Serrano-Ruiz *et al.* 2010). Technical lignin can be used in the preparation of carbon-based solid acid catalysts for its rich aromatic structure and oxygen-containing functional groups. In recent years, lignin has been studied as the carbon source for the preparation of carbon-based solid acids (Liang *et al.* 2013; Hu *et al.* 2015b; Li *et al.* 2018). However, the main problems encountered when using this substrate are the low specific surface area (12.07 m^2/g) and low acid density (0.37 mmol sulfonic groups/g catalyst) (Hu *et al.* 2015b). Moreover, the pore structure cannot be controlled without the use of template agents, and the amphiphilicity on the surface of the catalysts is not tunable, although the use of activators such as $ZnCl_2$, KOH, or K_2CO_3 can lead to a large specific surface area at a high temperature (600 to 900 °C) (Li *et al.* 2013; Hu *et al.* 2015b). It is known that mesoporous solid catalysts from carbon sources can be obtained *via* template methods, which use either hard SiO_2 surfaces (Huang *et al.* 2016), soft F127 surfaces (Libbrecht *et al.* 2017), or other template surfaces. However, the costs of the templates are too high for utilization at the industrial scale. The present study was conducted to obtain carbon-based solid acid catalysts derived from kraft lignin with a tunable textural structure, an amphiphilic surface, and a high total acid density at a more convenient cost.

Amphiphilic mesoporous carbon-based solid acid catalysts were prepared through the incomplete carbonization of kraft lignin with phosphoric acid that was then sulfonated with concentrated H_2SO_4. The catalysts were characterized and their catalytic activity for the hydration of α-pinene was compared with commercial solid acid catalysts, such as

Amberlyst-15 and strong mineral acids (*e.g.*, H_2SO_4). The catalysts obtained exhibited high catalytic activity due to the catalysts' high specific surface areas, high mesopores content, high total acid and sulfonic acid group density, and high amphiphilic activity. The current research presents a simple and efficient route to obtain carbon-based solid acid catalysts with tunable properties on a large scale. Such results have not been previously reported for carbonized kraft lignin, and could be interesting from the viewpoint of controlling the textural structure through adjusting the phosphoric acid dosage during the catalyst synthesis.

EXPERIMENTAL

Materials

Kraft lignin was isolated from the spent pulping liquor (*i.e.*, black liquor) of pine wood, which was provided by the Phoenix Pulp and Paper Co., Ltd. (Nanning, China). The α-Pinene was obtained from Wuzhou Sun Shine Forestry and Chemicals Co., Ltd. (Nanning, China). The chemical standards used in the gas chromatography (GC) analyses were all of chromatographic grade. Other chemicals and solvents used in this study were standard laboratory grade and were commercially obtained.

Methods

Catalyst preparation

Kraft lignin (10 g) was milled and sieved through a 100-mesh sieve to obtain a powder. Then, the sample was impregnated with a prescribed amount (10 g, 20 g, 30 g, or 40 g) of 85% phosphoric acid (analytical grade) while stirring overnight at room temperature with a magnetic stirrer. The impregnated sample was oven-dried at 110 °C for 12 h until a constant mass was achieved. The dried sample was transferred into a furnace with a nitrogen atmosphere where the temperature was increased from room temperature to 400 °C at a rate of 10 °C/min; the sample was maintained at 400 °C for 3 h under a nitrogen atmosphere. After activation and carbonization, the sample was washed with diluted hydrochloric acid and distilled water to remove impurities. After washing, the sample was oven-dried at 110 °C for 12 h to obtain the carbonized lignin (designated as LC_x, where 'x' is the phosphoric acid-to-lignin mass ratio). The sample LC_0 was synthesized under the same carbonization condition with no phosphoric acid impregnation.

Sulfonation was completed with 5 g LC_x immersed in 100 mL of 98% sulfuric acid and the mixture was stirred at 180 °C for 8 h. The sulfonated sample was washed with deionized water until the filtrate pH was 7.0, and the filtrate was tested with a barium chloride solution (0.10 mol/L) to ensure that free sulfuric acid was washed off absolutely. The washed sample was oven-dried under a vacuum at 60 °C for 12 h to obtain the carbon-based solid acid (LC_x-SO_3H).

Characterization of catalysts

Fourier transform infrared (FTIR) spectra of the samples were recorded using a Bruker Vector 33 spectrophotometer (Bruker Optics, Billerica, MA, USA) over the wavenumber range of 4,000 to 400 cm^{-1}.

X-ray diffraction (XRD) of the powdered samples was obtained using a Pgeneral XD-3 diffractometer (PERSEE, Beijing, China) equipped with a built-in recorder. The instrument used Cu-Kα radiation with a nickel filter, 30 Ma, and 40 kV. The scanning angle (2θ) that was used was between 5° and 65° with a scanning rate of 2°/min.

Raman spectra of the samples were recorded with an inVia Reflex spectrometer (Renishaw, Gloucestershire, UK) using a 532 nm wavelength.

Static contact angles of the samples were measured using water as the contact medium with a JY-82B contact angle meter (Beijing Harke Experimental Instruments, Beijing, China). The samples were pressed into sheets prior to the contact angle measurements.

The surface areas and porosities of the samples were characterized using the Brunauer-Emmitt-Teller (BET) isotherms that were performed at 77 K using a Micrometrics ASAP 2020 instrument (Micrometrics, Norcross, GA, USA) with nitrogen as the adsorbed gas. Prior to the BET isotherm measurements, all of the samples were degassed at 120 °C under a nitrogen atmosphere for 12 h.

Scanning electron microscope (SEM) images were taken using a Zeiss SUPRA 55 instrument equipped with a field emission electron gun (FEG) (Carl Zeiss Microscopy GmbH, Jena, Germany) and an energy dispersive spectrometer (EDS) (X-Max^{N}51-XMX1004; Oxford Instruments, Oxford, England). Samples were photographed after platinum spraying using an ion sputtering apparatus (GSL-1100X-SPC-16; Kejing Auto-Instrument Co., Ltd., Shenyang, China).

Thermogravimetric analysis (TGA) of the samples was performed using a TGA/SD T851e instrument (Mettler Toledo Ltd., Hong Kong, China). Analyses were conducted under a nitrogen atmosphere using a programmed heating rate of 10 °C /min from 0 °C to 1100 °C.

The adsorption capacities of the various catalysts for α-pinene were measured. A mixture of 4.00 g of α-pinene, 4.00 g of water, 20.00 mL of isopropanol, and 0.40 g of LC_x-SO_3H was added to a 50-mL conical flask that was then sealed. Next, the flask was placed in a SHZ-88 thermostat water bath oscillator (Hinotek Instrument Co., Ltd., Ningbo, China), the bath was operated at 150 rpm at 25 °C. An approximate 0.50 mL sample was removed from the flask at 2 h intervals. The sample was filtered using a 0.22-μm organic filter head, and the filtrate was collected for GC analysis. The amount of adsorption was calculated based on the analyses.

The acid densities of the various catalysts were determined *via* the acid-base titration method. This method was similar to that described by Toda *et al.* (2005) and Wang *et al.* (2011).

Catalytic testing

The activities of the synthesized solid acid catalysts for the hydration of α-pinene were measured. Briefly, a mixture of 20.00 mL isopropanol, 4.00 g α-pinene, 4.00 g distilled water, and 0.40 g LC_x-SO_3H catalyst was added to a 100-mL three-necked flask. The flask was placed in an oil bath, and the suspension was mixed with a magnetic stirrer (300 rpm) at 80 °C. A 0.50 mL sample was taken from the reaction mixture at specified time intervals. The aliquot was filtered through a 0.22-μm organic filter head to obtain a filtrate that was analyzed using GC. Catalytic experiments were also performed using commercially available Amberlyst-15 catalyst (53 m^2/g specific surface area, 4.70 mmol sulfonic acid groups/g catalyst, and 30 nm average pore diameter) and sulfuric acid catalyst respectively under the same conditions as those using the LC_x-SO_3H catalysts.

RESULTS AND DISCUSSION

Effect of Phosphoric Acid on Catalyst Preparation

Effect of phosphoric acid on carbonized kraft lignin

Effects of phosphoric acid dosages on the carbon yield from kraft lignin are shown in Table 1. When there was no phosphoric acid added, the carbon yield of LC_0 was only 52.4%. The carbon yield of the samples increased as the phosphoric acid dosages increased due to the dehydrolysis of the kraft lignin by phosphoric acid (Qin *et al.* 2014; Li *et al.* 2015). However, when a 4-to-1 phosphoric acid-to-lignin dosage was used, the carbon yield of LC_4 was slightly lower than that of LC_3. Higher phosphoric acid dosages not only increased the carbon yield from the kraft lignin, but they also affected the textural structure of the carbonized lignin. Phosphoric acid is a polar molecule and can penetrate into the lignin polymer to act as a plasticizer, to dehydrate at high temperatures, and to form melted microbeads. The following reactions are thought to occur with phosphoric acid (Li *et al.* 2015):

$$2H_3PO_4 \rightarrow H_4P_2O_7 + H_2O \quad (1)$$

$$3H_3PO_4 \rightarrow H_5P_3O_{10} + 2H_2O \quad (2)$$

$$nH_3PO_4 \rightarrow H_{n+2}P_nO_{3n+1} + (n - 1)H_2O \quad (3)$$

As shown in Fig. 1, phosphoric acid reacted with lignin to form phosphate linkages, such as phosphate and polyphosphate esters (Jagtoyen and Derbyshire 1998; Li *et al.* 2015). After phosphoric acid carbonization, the phosphate lignin derivatives were dissolved during washing with dilute hydrochloric acid and deionized water. This resulted in a solid carbonized material with a complex pore structure.

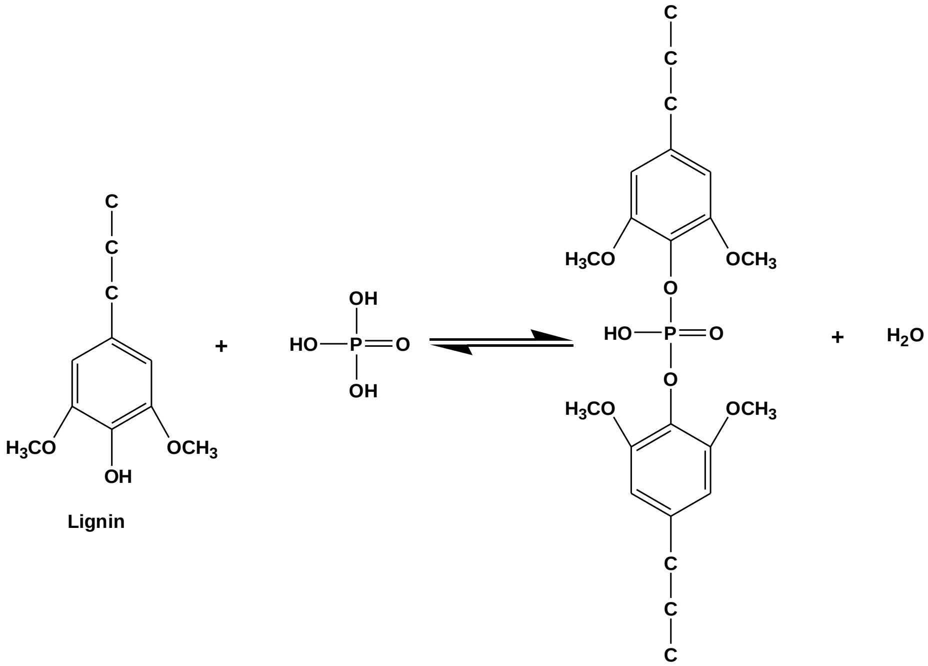

Fig. 1a. Postulated phosphate ester formation by the phosphorylation of lignin

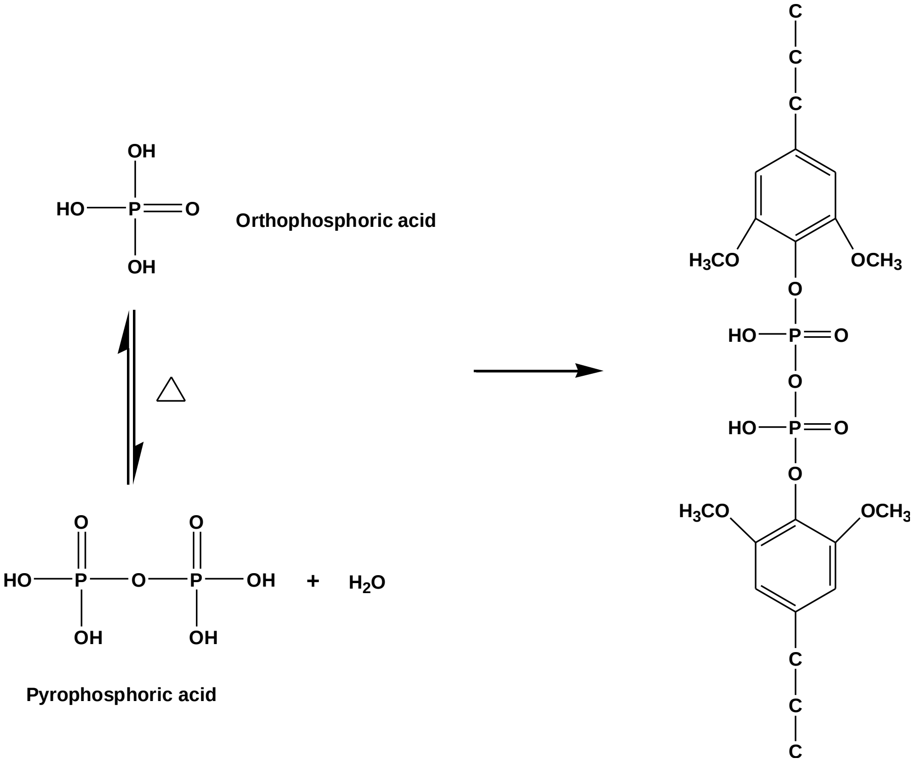

Fig. 1b. Postulated phosphate ester formation by the phosphorylation of lignin

The micropore volumes of LC_2, LC_3, and LC_4 were similar to one another (approximately 0.12 cm^3/g); however, the mesoporous volume (V_{meso}) values of the samples were different (Table 1). Generally, as the phosphoric acid dosage increased, the V_{meso} of the carbonized lignin increased. Conversely, with a further increase in phosphoric acid dosage, the interconnection between the mesopore with other mesopore led to the formation of invalid large holes, which led to a decreased mesoporous volume. The specific surface area (S_{BET}), pore volume (V_p), and average pore diameter (D_p) of LC_0 and LC_1 were too small to be measured using the BET isotherm method. When the phosphoric acid dosage was three times that of lignin, the specific surface area, pore volume, and average pore diameter of the carbonized material increased to 844.02 m^2/g, 0.87 cm^3/g, and 6.57 nm, respectively; likewise, the mesoporous ratio of LC_3 increased to 86.2%.

Table 1. Surface and Textural Characteristics of Carbonized Kraft Lignin

Sample	Carbon Yield (%)	S_{BET} [a] (m^2/g)	V_p [b] (cm^3/g)	V_{meso} [c] (cm^3/g)	D_p [d] (nm)	Mesoporous Ratio [e] (%)
LC_0	52.4	-	-	-	-	-
LC_1	55.3	-	-	-	-	-
LC_2	63.3	660.22	0.52	0.40	5.14	76.9
LC_3	65.7	844.02	0.87	0.75	6.57	86.2
LC_4	64.2	703.03	0.55	0.43	5.00	78.2

[a] Specific surface area; [b] total pore volume; [c] mesoporous volume; [d] average pore diameter; and [e] mesoporous ratio = (mesoporous volume / total pore volume) • 100

Effect of phosphoric acid treatment on carbonized lignin acid catalysts

The surface and textural characteristics of catalysts are presented in Table 2. When no phosphoric acid was used as an activator, the specific surface area of LC_0-SO_3H was low (0.17 m^2/g). As the amount of phosphoric acid increased, the specific surface area and pore volume of the catalysts increased. When the phosphoric acid-to-lignin ratio was 3-to-1, the specific surface area and pore volume of the catalyst peaked at 282.2 m^2/g and 0.26 cm^3/g, respectively. These observed trends with LC_x-SO_3H were basically consistent with those of the carbonized lignin (LC_x). However, the specific surface area of LC_x-SO_3H was lower than the corresponding LC_x, which was attributed to the sulfonation reaction (Ogino *et al.* 2015). It was noted that the specific surface area of LC_0-SO_3H and LC_1-SO_3H increased when compared to LC_0 and LC_1, respectively, which indicated that the sulfonation reaction created new pore structures in carbonized lignin that had little to no modification by the phosphoric acid. The specific surface area of LC_4-SO_3H was close to that of LC_3-SO_3H, but the average pore volumes and average pore diameters decreased; this observation implied that the mesoporous structure of LC_4-SO_3H was negatively altered, which drastically lowered the mesoporous ratio of LC_4-SO_3H.

Table 2. Surface and Textural Characteristics of Carbonized Kraft Lignin Catalysts After Sulfonation When Compared to Amberlyst-15

Sample	S_{BET} [a] (m^2/g)	V_p [b] (cm^3/g)	V_{meso} [c] (cm^3/g)	D_p [d] (nm)	M_r [e] (%)	A_c [f] (mg/g)	Acid Density [g] (mmol/g)			
							-SO_3H	-COOH	-OH	Total
LC_0-SO_3H	0.17	-	-	-	-	120	0.38	1.68	1.18	3.24
LC_1-SO_3H	88.42	0.09	0.07	7.17	77.8	179	0.48	2.11	1.65	4.24
LC_2-SO_3H	129.16	0.12	0.09	6.69	75.0	439	0.55	2.23	1.86	4.64
LC_3-SO_3H	282.20	0.26	0.19	6.73	73.1	663	0.57	2.35	1.91	4.83
LC_4-SO_3H	257.72	0.16	0.08	3.74	50.0	589	0.48	2.27	1.77	4.52
Amberlyst-15	53.00	-	-	30.0	-	424	4.70	-	-	4.70

[a] Specific surface area; [b] total pore volume; [c] mesoporous volume; [d] average pore size; [e] mesoporous ratio = (mesoporous volume / total pore volume) • 100; [f] adsorption capacity of *α*-pinene; and [g] based on acid-base titration

The acid density values for the various LC_x-SO_3H catalysts are also shown in Table 2. As the phosphoric acid dosage during lignin carbonization increased, the densities of sulfonic (-SO_3H), carboxylic (-COOH), phenolic (-OH), and total acid for the carbonized catalysts also increased. These acid density values reached their maximum value when the phosphoric acid-to-lignin ratio was 3-to-1 (*i.e.*, LC_3-SO_3H). The acid density was related to the textural structure of the carbonized lignin. When the specific surface area was higher, there was more oxidation and sulfonation of the surfaces of the carbonized lignin. The phosphoric acid activator added during the carbonization might also promote the formation of carboxylic and phenolic groups (Lin *et al.* 2019). The sulfonic acid density of LC_3-SO_3H was also measured using energy dispersive X-ray spectroscopy (EDS) and the value obtained (0.53 mmol/g) was similar to the value obtained *via* the acid-base titration method (*i.e.*, 0.57 mmol/g).

Images from the contact angle measurements are shown in Fig. 2. The contact angles (CA) of LC_0-SO_3H and LC_3-SO_3H were 121.0° and 14.3°, respectively. These observations indicated that LC_0-SO_3H had a hydrophobic surface, whereas LC_3-SO_3H had a hydrophilic surface due to the presence of polar sulfonic, carboxylic, and phenolic groups. The *α*-pinene adsorption capacity (A_c) of the samples increased as the phosphoric acid activator dosage increased (Fig. 3). When the phosphoric acid-to-lignin dosage was greater than 2-to-1, the A_c of the resulting LC$_x$-SO$_3$H increased. Under the same conditions, the larger surface area of a catalyst has, the larger A_c of *α*-pinene has. Hence, LC$_3$-SO$_3$H had amphiphilic characteristics towards hydrophobic (*e.g.*, *α*-pinene) and hydrophilic (*e.g.*, water) molecules. Properties, such as amphiphilic nature, high specific surface area, high sulfonic acid group density, and high mesoporous ratio, should make LC$_3$-SO$_3$H an effective hydration catalyst for *α*-pinene.

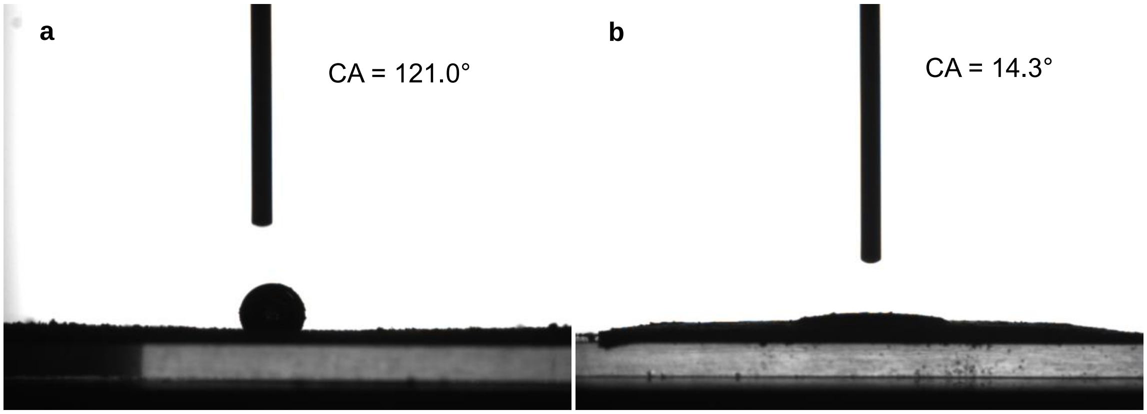

Fig. 2. Contact angles of LC$_0$-SO$_3$H (a), LC$_3$-SO$_3$H (b)

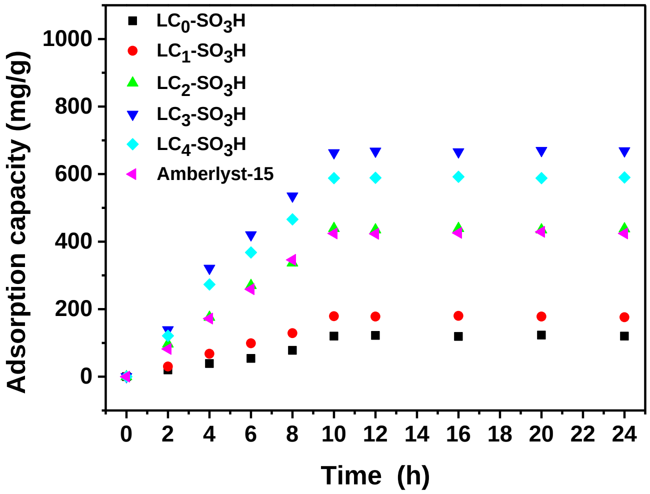

Fig. 3. *α*-Pinene adsorption capacity of LC$_x$-SO$_3$H

Pseudo-first-order and pseudo-second-order kinetic equations for the adsorption capacity of *a*-pinene on catalysts were fitted. Fitting results are shown in Fig. 4, and the adsorption kinetic rate constants and R^2 of the catalysts are shown in Table 3. From Table 3, it can be seen that the adsorption of *α*-pinene on the catalysts were well fitted with the pseudo-first-order kinetics. Furthermore, LC$_3$-SO$_3$H had the largest rate constant among all the catalysts. This is because LC$_3$-SO$_3$H had the largest specific surface area and mesoporous volume, which is conducive to the adsorption and mass transfer during the reaction.

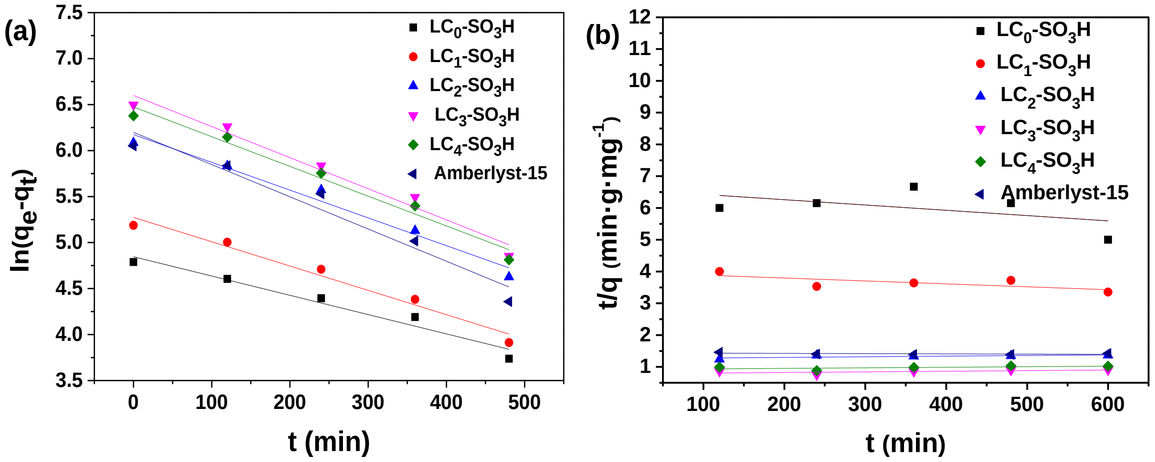

Fig. 4. Pseudo-first-order kinetic fitting curves (a) and pseudo-second-order kinetic fitting curves (b) of *α*-pinene adsorption on catalysts

Table 3. Fitting Results of Adsorption Kinetics for *α*-Pinene onto Catalysts

Sample	Pseudo-first-order-model		Pseudo-second-order-model	
	k_1 (min^{-1})	R^2	k_2 (g·mg^{-1}·min^{-1})	R^2
LC$_0$-SO$_3$H	0.0021	0.9466	0.0016	0.0237
LC$_1$-SO$_3$H	0.0026	0.9654	0.0009	0.3720
LC$_2$-SO$_3$H	0.0030	0.9650	0.0002	0.3457
LC$_3$-SO$_3$H	0.0034	0.9645	0.0002	0.1255
LC$_4$-SO$_3$H	0.0032	0.9687	0.0002	0.0808
Amberlyst-15	0.0030	0.9377	0.0001	0.0230

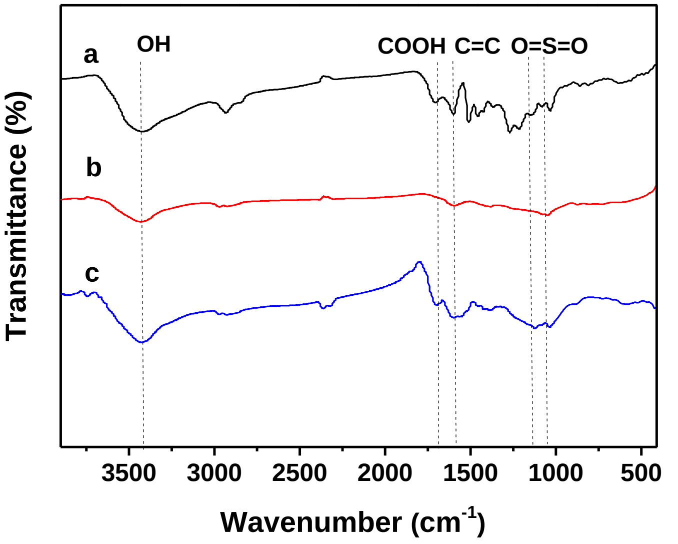

Fig. 5. FTIR spectra: (a) lignin; (b) LC$_3$; and (c) LC$_3$-SO$_3$H

Characterization of Catalysts

FTIR analysis

The FTIR spectra of lignin, LC$_3$, and LC$_3$-SO$_3$H are shown in Fig. 5. The broad absorption band around 3420 cm^{-1} is ascribed to the hydroxyl stretching vibration. The peaks at 1165 cm^{-1} and 1030 cm^{-1} were attributed to symmetric and asymmetric stretching vibrations of O=S=O. This observation indicated that sulfonic acid groups were successively incorporated onto the solid catalyst (Song *et al.* 2012; Konwara *et al.* 2018). The band at 1600 cm^{-1} was assigned to C=C stretching vibrations in aromatic carbons. The band at 1710 cm^{-1} was attributed to a C=O bending vibration (Shen *et al.* 2013), which indicated the presence of carboxylic acid groups on the LC_3-SO_3H catalyst.

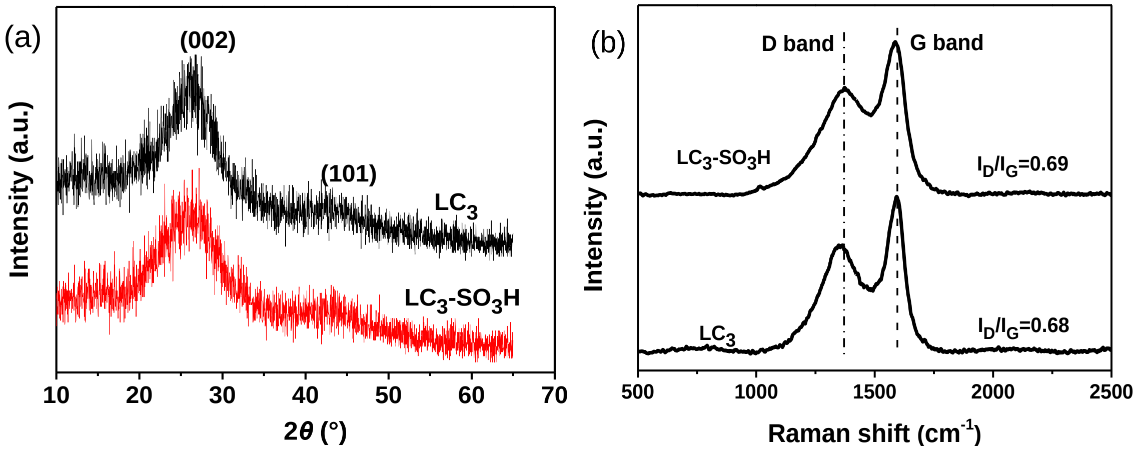

Fig. 6. XRD spectra (a) of LC_3 and LC_3-SO_3H; and Raman spectra (b) of LC_3 and LC_3-SO_3H

XRD and Raman spectroscopy analyses

Figure 6 illustrates the XRD and Raman spectra obtained from LC_3 and LC_3-SO_3H. The XRD of LC_3 and LC_3-SO_3H exhibited two broad diffraction peaks (2θ) at 10° to 30° and 30° to 50°, which corresponded to a carbon structure comprised of randomly-oriented sheets of polycyclic aromatic carbons (Qin *et al.* 2014). The Raman spectra collaborated the findings from the XRD analyses and Raman scattering peaks were observed at 1361 cm^{-1} (D band) and 1593 cm^{-1} (G band), which indicated polycyclic aromatic carbon sheets were present (Song *et al.* 2015). The ratio of D-to-G bands (I_D/I_G) of LC_3 and LC_3-SO_3H were 0.68 and 0.69, respectively. The I_D/I_G values were not high because of the relatively low temperature (400 °C) used during the lignin carbonization process.

BET isotherm analyses

Figure 7(a) shows the BET isotherms of all samples were type IV with H3 hysteresis loops. The curves at a relative pressure ratio of 0.30 to 0.90 can be classified as typical mesoporous materials, whereas a relative pressure ratio greater than 0.90 can be assigned to multilayer nitrogen adsorption by the macropores (Tian *et al.* 2017). The pore size distribution curves of the LC_x-SO_3H catalysts are shown in Fig. 7(b). The pore sizes of the LC_x-SO_3H catalysts were mainly mesoporous (2 to 50 nm). In contrast, the LC_3-SO_3H catalyst had some macropores, whereas the LC_4-SO_3H catalyst had almost no macropores. The LC_1-SO_3H, LC_2-SO_3H, and LC_3-SO_3H had a uniform pore size distribution, whereas LC_4-SO_3H possessed a different distribution. Therefore, the application of an appropriate phosphoric acid dosage during lignin carbonization can effectively maximize the porosity of the solid acid catalyst to obtain higher mesopore volume and ratio values.

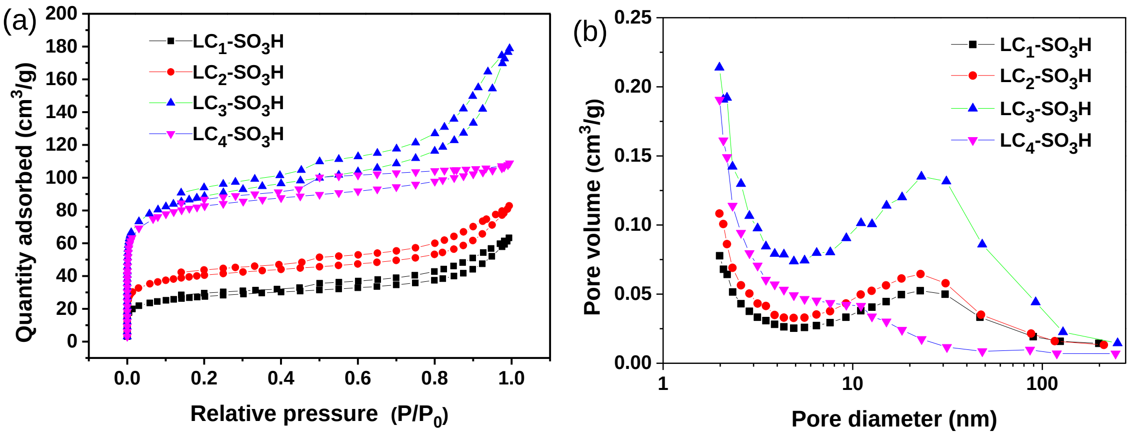

Fig. 7. BET adsorption isotherms (a) and pore size distribution curves (b) of LC_x-SO_3H

SEM analysis

The morphologies of the carbonized lignins and the prepared catalysts are shown in Fig. 8.

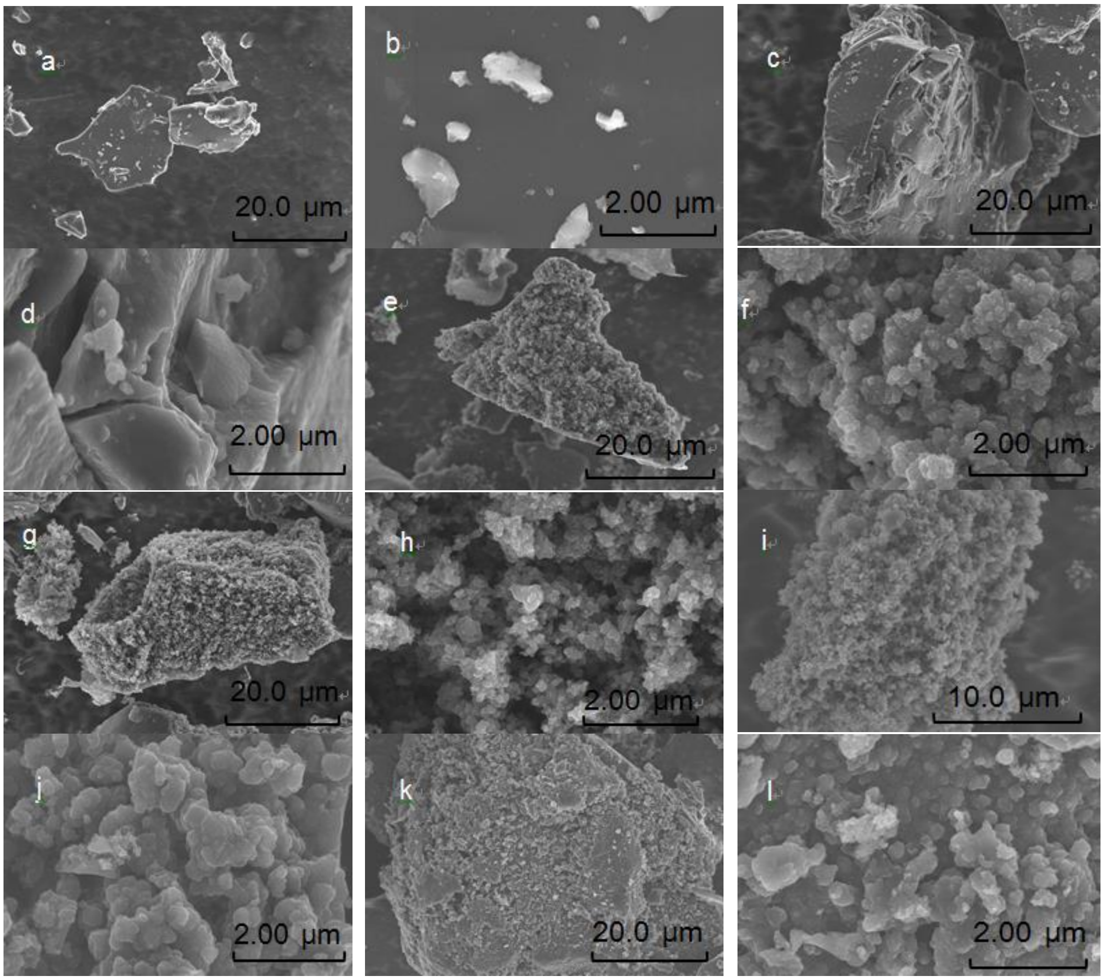

Fig. 8. SEM images of carbonized lignin samples: LC_0 (a and b); LC_1 (c and d); LC_2 (e and f); LC_3 (g and h); LC_4 (i and j); and LC_3-SO_3H (k and l)

The SEM images showed that the surfaces of LC_0 and LC_1 were flat and smooth. However, LC_2, LC_3, LC_4, and LC_3-SO_3H had irregular surfaces with well-developed coralloid porous structures. These observations indicated that the samples without phosphoric acid activation (LC_0) or little phosphoric acid activation (LC_1) had no porous development during lignin carbonization. When LC_3 was compared with LC_3-SO_3H, it was observed that the LC_3-SO_3H sample had lower porosity than the LC_3 sample. This indicated that a portion of the pore structure was altered during the sulfonation of the carbonized lignin, but the morphological structure of the catalyst was almost the same as that of the original carbonized lignin. The phenomena shown in the SEM images were consistent with the experimental data obtained from the BET isotherms.

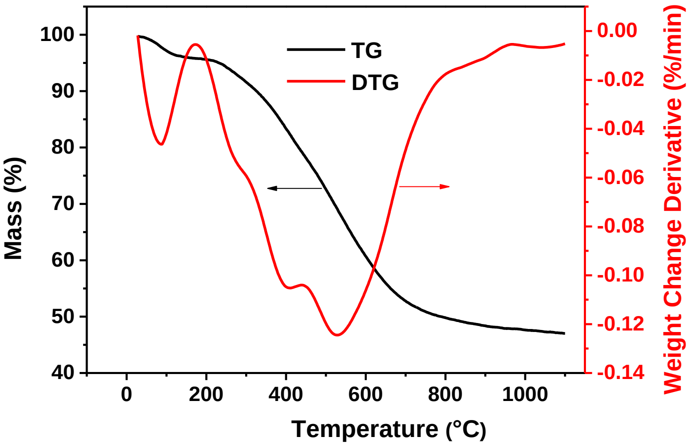

Fig. 9. TG and DTG curves of LC_3-SO_3H catalyst

TG and DTG analyses

The thermal stability of LC_3-SO_3H was characterized by thermogravimetric (TG) and differential thermogravimetric (DTG) analyses (Fig. 9). The observed mass loss (approximately 5%) at temperatures below 120 °C is attributed to moisture losses. There were almost no mass losses at temperatures between 120 to 250 °C, which suggested that the LC_3-SO_3H catalyst possessed high thermal stability, and could be used at temperatures below 250 °C. Approximately 45% mass loss of the LC_3-SO_3H catalyst occurred between 250 to 800 °C, which was attributed to the loss of volatiles and tar from the sample.

Catalytic Activities

Catalytic mechanism and performance

The postulated mechanism of the hydration of α-pinene *via* the carbon-based solid acid catalyst is shown in Fig. 10. The pinane carbocation intermediate was formed *via* the electrophilic addition of α-pinene with a proton from the sulfonic acid group on the catalyst surface. Then, the pinane carbocation intermediate underwent a ring opening reaction of its bicyclic structure to form another carbocation intermediate. Finally, the nucleophilic addition of water to the carbocation intermediate formed α-terpineol, along with the protonation of the sulfite group at the catalyst's surface. For a heterogeneous catalysis system, the reaction takes place on the solid surface of the catalyst. Adequate specific surface areas for a catalyst with abundant active sites play an important role in catalytic reactions. It is also important that the reactant can be adsorbed onto the surface of a catalyst. In addition, diffusion and mass transfer phenomena are important factors with a heterogeneous catalytic system. The synthesis of *α*-terpineol by the hydration of *α*-pinene, as described in this study, is an acid-catalyzed heterogeneous process. The performances of the different solid acid catalysts are compared in Table 4.

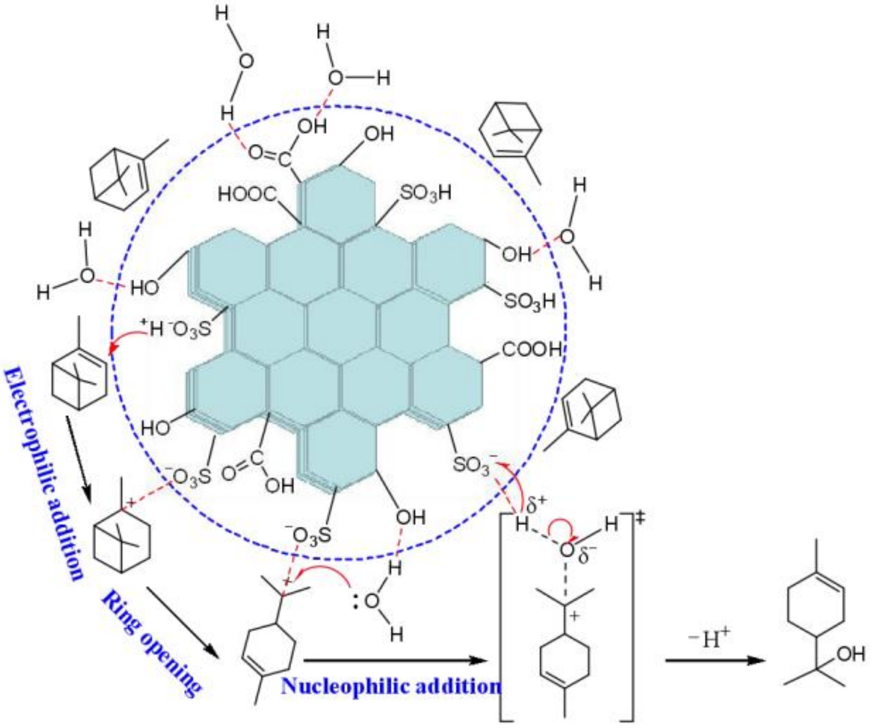

Fig. 10. Postulated catalytic reaction mechanism for *α*-terpineol synthesis when using the solid acid catalyst derived from carbonized lignin after sulfonation

Table 4. Performance of Solid Acid Catalysts in the Hydration of *α*-Pinene

Sample	Conversion ^{a} (%)	Yield ^{b} (%)	Selectivity ^{c} (%)
LC_0-SO_3H	65.3	22.4	34.3
LC_1-SO_3H	87.4	37.2	42.6
LC_2-SO_3H	93.1	43.1	46.3
LC_3-SO_3H	95.3	55.3	58.1
LC_4-SO_3H	93.9	43.1	45.9
Amberlyst-15	97.4	34.4	35.3
H_2SO_4 ^{d}	85.5	36.7	42.9
H_2SO_4 ^{e}	96.9	41.5	42.8
H_2SO_4 ^{f}	97.3	39.8	40.9

^{a} Conversion of *α*-pinene; ^{b} yield of *α*-terpineol; ^{c} selectivity of *α*-terpineol; ^{d} The total acidity value of sulfuric acid is equal to the total acidity value of 0.20g LC_3-SO_3H; ^{e} The total acidity value of sulfuric acid is equal to the total acidity value of 0.40g LC_3-SO_3H; and ^{f} The total acidity value of sulfuric acid is equal to the total acidity value of 0.80g LC_3-SO_3H.

The LC_3-SO_3H had a high surface area that possessed hydrophobic and hydrophilic regions that allowed the solid acid catalyst to adsorb high amounts of *α*-pinene and water onto its surfaces such that they could react with one another. Furthermore, the high acid density (-SO_3H) of LC_3-SO_3H provided adequate active sites for the catalytic reactions to occur. Additionally, the abundant mesoporous and macroporous structures of LC_3-SO_3H facilitated diffusion and mass transfer phenomena to occur. These particular properties of LC_3-SO_3H made it an effective acid catalyst for synthesizing *α*-terpineol. It was found that the catalytic performance of LC_0-SO_3H was poor due to its low specific surface area, low amphiphilicity, and low sulfonic acid density. Both LC_2-SO_3H and LC_3-SO_3H had almost the same conversion levels of *α*-pinene to *α*-terpineol, but the yields of *α*-terpineol were quite different for these two acid catalysts. The yield from LC_3-SO_3H was much higher than that from LC_2-SO_3H, which could have been due to LC_3-SO_3H having a higher specific surface area and higher pore volume than LC_2-SO_3H. Both LC_3-SO_3H and LC_4-SO_3H had almost the same specific surface areas; however, the catalytic performance of LC_3-SO_3H was much higher than that of LC_4-SO_3H. Two possible reasons for this observation could have been related to the total acid density of LC_3-SO_3H being higher than that of LC_4-SO_3H, or to more abundant mesoporous and macroporous structures in LC_3-SO_3H than in LC_4-SO_3H (which affected diffusion and mass transfer phenomena). The LC_2-SO_3H had a higher sulfonic acid density, a larger average pore size, and a higher mesoporous ratio than LC_4-SO_3H, but had a lower specific surface area; however, both of these acid catalysts had similar performances. The *α*-pinene conversion was high when Amberlyst-15 was used as the acid catalyst, but the *α*-terpineol yield was not as high. Amberlyst-15 had a high sulfonic acid group density but did not have other polar functional groups, such as carboxylic and phenolic groups, which negatively affected the amphiphilic nature of the catalyst's surface. This caused the Amberlyst-15 catalyst to form more isomerized reaction products from *α*-pinene. The above observations indicated that the performance of a solid acid catalyst was affected by several factors, such as acid density, specific surface area, porosity, amphiphilic nature, *etc*. Fortunately, the catalytic performance was controlled through adjusting the phosphoric acid dosage used during lignin carbonization. When LC_3-SO_3H was used as the solid acid catalyst, the *α*-pinene conversion and the *α*-terpineol yield were 95.26% and 55.32%, respectively. These results were much better than those obtained from sulfuric acid as a catalyst (Table 4).

Optimization of the α-pinene hydration reaction

The effect of reaction conditions on the hydration of *α*-pinene using LC_3-SO_3H as the solid acid catalyst is shown in Fig. 11. The catalyst dosage had little effect on its catalytic performance. Under the same experimental conditions, when the catalyst dosage was higher than 0.40 g, the conversion value remained almost constant, but the *α*-terpineol yield slightly decreased (Fig. 11(a)). This discrepancy may have been caused by stirring, which affected the diffusion process. The reaction temperature had an appreciable influence on the catalytic performance (Fig. 11(b)). When the other reaction conditions were held constant, the yield of *α*-terpienol increased as the reaction temperature increased from 65 to 80 °C. The hydration reaction of *α*-pinene is a reversible exothermic reaction, but the molecular activation requires a certain amount of energy to occur. Therefore, increasing the reaction temperature was beneficial to the formation of *α*-terpineol. Moreover, it can be seen from Fig. 11(c) that the water loading also affected the hydration of *α*-pinene. When the other reaction conditions were held constant, adjusting the molar ratio of water-to-isopropanol (while the total volume was kept constant) marginally affected the conversion of *α*-pinene. Nonetheless, the *α*-terpineol yield initially increased and then appreciably decreased. This observation was explained by competitive isomerization reactions occurring, as well as the formation of undesirable byproducts, such as camphene, limonene, *α*-terpinolene and terpini hydras (Yang *et al.* 2011; Prakoso *et al.*

2018). The isomerization reactions were considerable when the water loading level was insufficient. However, excess water loading level can lead to non-uniform reactions that afford other undesired terpineol products. Both reaction condition extremes reduced the α-terpineol yield.

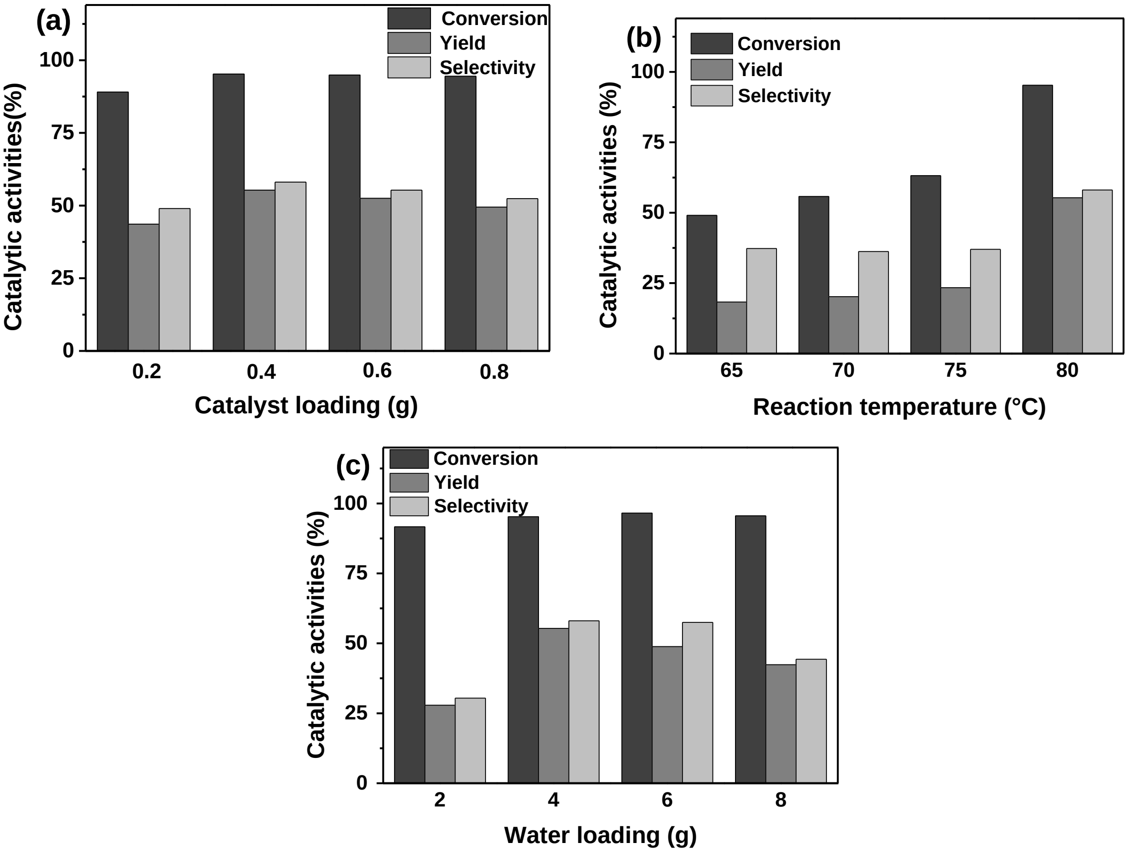

Fig. 11. Performance of LC_3-SO_3H as catalyst: (a) effect of catalyst dosage at 80 °C and 4.00 g of water; effect of reaction temperature at 0.4 g of LC_3-SO_3H catalyst and 4.00 g of water; and (c) effect of water loading at 80 °C and 0.4 g of LC_3-SO_3H catalyst; other reaction conditions were held constant: 4.00 g of α-pinene, 20.00 mL of isopropanol as solvent, and 24 h reaction time.

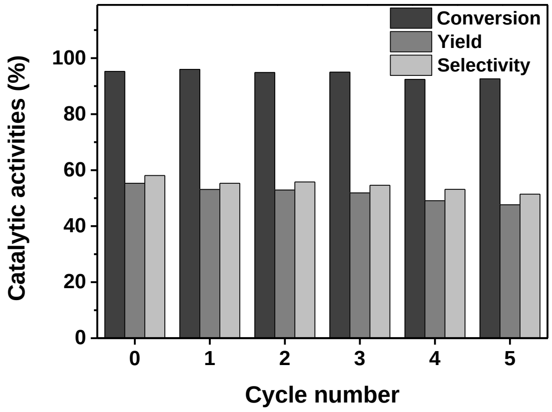

Fig. 12. Performance of LC_3-SO_3H as a catalyst when recovered and recycled; reaction conditions were: 4.00 g of α-pinene and 4.00 g of water as raw materials; 20.00 mL of isopropanol as solvent; 0.40 g of LC_3-SO_3H as catalyst; reaction temperature of 80 °C; and reaction time of 24 h

Catalyst recycling

The recyclability of the solid acid catalyst, LC_3-SO_3H, was examined. The catalyst was separated from the hydration reaction products *via* filtration. Afterwards, the used catalyst was repeatedly rinsed with ethanol and deionized water. After washing, the catalyst was oven-dried overnight at 120 °C. The dry catalyst was then used under the same conditions as before, and its catalytic performance was re-evaluated (Fig. 12). The reusability of the catalyst was excellent. After 5 cycles without regeneration the conversion of *α*-pinene and the yield of *α*-terpineol slightly decreased from 95.3% to 92.6% and from 55.3% to 47.6%, respectively. This observed result may have been caused by the loss of some acid reaction sites and by the blockage of some pores of the catalyst each time it was recycled.

CONCLUSIONS

1. A solid acid catalyst was prepared from carbonized kraft lignin that was activated by phosphoric acid. The resulting catalyst was amphiphilic, mesoporous, and carbon-based. The pore structure and surface amphiphilicity of the catalyst can be adjusted by changing the phosphoric acid dosages to yield a solid with high specific surface area, high surface amphiphilicity, high mesoporous ratio, and high acid density. Moreover, the method used to produce the solid acid catalyst was low cost and simple. The acid density, specific surface area, porosity, and surface amphiphilicity affected the catalytic hydration reaction of *α*-pinene.
2. The effects of different factors on the hydration reaction of α-pinene were studied. Under the optimum conditions, the performance of the carbonized lignin catalyst was better than sulfuric acid and Amberlyst-15. The conversion of *α*-pinene and the yield of *α*-terpineol were as high as 95.3% and 55.3%, respectively, when using the carbonized lignin catalyst. In addition, the carbonized lignin catalyst could be recovered and reused five times without appreciably decreasing its catalytic performance (*i.e*., 92.6% *α*-pinene conversion and 47.6% *α*-terpineol yield.)

ACKNOWLEDGMENTS

The authors acknowledge the financial support from the National Natural Science Foundation of China (Grant No. 31660180), and the Innovation Project of Guangxi Graduate Education (gxun-chxzs 2017133).

REFERENCES CITED

Avila, M. C., Comelli, N. A., Firpo, N. H., Ponzi, E. N., and Ponzi, M. I. (2008). “Hydration and acetylation of limonene: Supported heteropolyacids,” *J. Chil. Chem. Soc.* 53(1), 1449-1451. DOI: 10.4067/s0717-97072008000100027

Bedia, J., Ruiz-Rosas, R., Rodríguez-Mirasol, J., and Cordero, T. (2010). “A kinetic study of 2-propanol dehydration on carbon acid catalysts,” *J. Catal.* 271(1), 33-42. DOI: 10.1016/j.jcat.2010.01.023

Budarin, V., Clark, J. H., Hardy, J. J. E., Luque, R., Milkowski, K., Tavener, S. J., and Wilson, A. J. (2006). "Starbons: New starch-derived mesoporous carbonaceous materials with tunable properties," *Angew. Chem. Int. Edit.* 45(23), 3782-3786. DOI: 10.1002/anie.200600460

Erman, W. F. (1985). *Chemistry of the Monoterpenes*, Marcel Dekker, New York, NY, USA.

Ezebor, F., Khairuddean, M., Abdullah, A. Z., and Boey, P. L. (2014). "Oil palm trunk and sugarcane bagasse derived solid acid catalysts for rapid esterification of fatty acids and moisture-assisted transesterification of oils under pseudo-infinite methanol," *Bioresource Technol*. 157, 254-262. DOI: 10.1016/j.biortech.2014.01.110

Fukuhara, K., Nakajima, K., Kitano, M., Kato, H., Hayashi, S., and Hara, M. (2011). "Structure and catalysis of cellulose-derived amorphous carbon bearing SO_3H groups," *ChemSusChem* 4(6), 778-784. DOI: 10.1002/cssc.201000431

Geng, L., Wang, Y., Yu, G., and Zhu, Y. (2011). "Efficient carbon-based solid acid catalysts for the esterification of oleic acid," *Catal. Commun*. 13(1), 26-30. DOI: 10.1016/j.catcom.2011.06.014

Gosselink, R. J. A., Jong, E., Guran, B., and Abächerli, A. (2004). "Co-ordination network for lignin-standardization, production and applications adapted to market requirements (EUROLIGNIN)," *Ind. Crop. Prod*. 20(2), 121-129. DOI: 10.1016/j.indcrop.2004.04.015

Hara, M., Yoshida, T., Takagaki, A., Takata, T., Kondo, J. N., Hayashi, S., and Dome, K. (2004). "A carbon material as a strong protonic acid," *Angew. Chem. Int. Edit*. 43(22), 2955-2958. DOI: 10.1002/ange.200453947

Haziratul Mardhiah, H., Ong, H. C., Masjuki, H. H., Lim, S., and Pang, Y. L. (2017). "Investigation of carbon-based solid acid catalyst from *Jatropha curcas* biomass in biodiesel production," *Energ. Convers. Manage*. 144, 10-17. DOI: 10.1016/j.enconman.2017.04.038

Hu, L., Lin, L., Wu, Z., Zhou, S., and Liu, S. (2015a). "Chemocatalytic hydrolysis of cellulose into glucose over solid acid catalysts," *Appl. Catal. B- Environ*. 174-175, 225-243. DOI: 10.1016/j.apcatb.2015.03.003

Hu, S., Jiang, F., and Hsieh, Y. (2015b). "1D lignin-based solid acid catalysts for cellulose hydrolysis to glucose and nanocellulose," *ACS Sustain. Chem. Eng.* 3(10), 2566-2574. DOI: 10.1021/acssuschemeng.5b00780

Huang, A., Zhu, X., Wang, S., Tian, Y., and Wang, X. (2016). "Synthesis of bimodal mesoporous carbon spheres from biomass starch and CBZ release," *Mater. Lett.* 169, 54-57. DOI: 10.1016/j.matlet.2016.01.075

Jagtoyen, M., and Derbyshire, F. (1998). "Activated carbons from yellow poplar and white oak by H_3PO_4 activation," *Carbon* 36(7-8), 1085-1097. DOI: 10.1016/S0008-6223(98)00082-7

Konwara, L. J., Samikannua, A., Mäki-Arvelab, P., Boströmc, D., and Mikkola, J. (2018). "Lignosulfonate-based macro/mesoporous solid protonic acids for acetalization of glycerol to bio-additives," *Appl. Catal. B- Environ.* 220, 314-323. DOI: 10.1016/j.apcatb.2017.08.061

Li, X., Zuo, Y., Zhang, Y., Fu, Y., and Guo, Q. (2013). "*In situ* preparation of K_2CO_3 supported kraft lignin activated carbon as solid base catalyst for biodiesel production," *Fuel* 113, 435-442. DOI: 10.1016/j.fuel.2013.06.008

Li, Y., Shen, S., Wang, C., Peng, X., and Yuan, S. (2018). "The effect of difference in chemical composition between cellulose and lignin on carbon based solid acids applied for cellulose hydrolysis," *Cellulose* 25(3), 1-13. DOI: 10.1007/s10570-018-1693-7

Li, Y., and Zeng, D. (2017). "Synthesis and characterization of flower-like carbon spheres solid acid from glucose for esterification," *Mater. Lett.* 193, 172-175. DOI: 10.1016 /j.matlet.2017.01.071

Li, Y., Zhang, X., Yang, R., Li, G., and Hu, C. (2015). "The role of H_3PO_4 in the preparation of activated carbon from NaOH-treated rice husk residue," *RSC Adv.* 5(41), 32626-32636. DOI: 10.1039/c1gc15306d

Liang, F., Song, Y., Huang, C., Zhang, J., and Chen, B. (2013). "Preparation and performance evaluation of a lignin-based solid acid from acid hydrolysis lignin," *Catal. Commun*. 40, 93-97. DOI: 10.1016/j.catcom.2013.06.005

Libbrecht, W., Verberckmoes, A., Thybaut, J. W., Voort, P. V. D., and Clercq, J. D. (2017). "Soft templated mesoporous carbons: Tuning the porosity for the adsorption of large organic pollutants," *Carbon* 116, 528-546. DOI: 10.1016/j.carbon.2017.02.016

Lin, Q., Zhang, C., Wang, X., Cheng, B., Mai, N., and Ren, J. (2019). "Impact of activation on properties of carbon-based solid acid catalysts for the hydrothermal conversion of xylose and hemicelluloses," *Catal. Today* 319, 31-40. DOI: 10.1016/j.cattod.2018.03.070

Liu, F., Zheng, A., Noshadi, I., and Xiao, F. S. (2013). "Design and synthesis of hydrophobic and stable mesoporous polymeric solid acid with ultra strong acid strength and excellent catalytic activities for biomass transformation," *Appl. Catal. B-Environ.* 136-137, 193-201. DOI: 10.1016/j.apcatb.2013.01.063

Liu, Z., Lu, X., An, L., and Xu, C. (2016). "A novel cationic lignin-amine emulsifier with high performance reinforced *via* phenolation and Mannich reactions," *BioResources* 11(3), 6438-6451. DOI: 10.15376/biores.11.3.6438-6451

Malins, K., Kampars, V., Brinks, J., Neibolte, I., and Murnieks, R. (2015). "Synthesis of activated carbon based heterogenous acid catalyst for biodiesel preparation," *Appl. Catal. B- Environ.* 176-177, 553–558. DOI: 10.1016/j.apcatb.2015.04.043

Ogino, I., Suzuki, Y., and Mukai, S. R. (2015). "Tuning the pore structure and surface properties of carbon-based acid catalysts for liquid-phase reactions," *ACS Catal*. 5(8), 4951-4958. DOI: 10.1021/acscatal.5b01022

Okuhara, T. (2002). "Water-tolerant solid acid catalysts," *Chem. Rev*. 102(10), 3641-3666. DOI: 10.1002/chin. 200303268

Pakdel, H., Sarron, S., and Roy, C. (2001). "*α*-Terpineol from hydration of crude sulfate turpentine oil," *J. Agr. Food Chem*. 49(9), 4337-4341. DOI: 10.1021/jf010341b

Prakoso, T., Hanley, J., Soebianta, M. N., and Soerawidjaja, T. H. (2018). "Synthesis of terpineol from *α*-pinene using low-price acid catalyst," *Catal. Lett*. 148(2), 725-731. DOI: 10.1007/s10562-017-2267-2

Qi, W., He, C., Wang, Q., Liu, S., Yu, Q., Wang, W., Leksawasdi, N., Wang, C., and Yuan, Z. (2018). "Carbon-based solid acid pretreatment in corncob saccharification: Specific xylose production and efficient enzymatic hydrolysis," *ACS Sustain. Chem. Eng.* 6(3), 3640-3648. DOI: 10.1021/acssuschemeng.7b03959

Qin, C., Chen, Y., and Gao, J. (2014). "Manufacture and characterization of activated carbon from marigold straw (*Tagetes erecta* L) by H_3PO_4 chemical activation," *Mater. Lett.* 135, 123-126. DOI: 10.1016/j.matlet.2014.07.151

Robles-Dutenhefner, P. A., Silva, K. A., Siddiqui, M. R. H., Kozhevnikov, I. V., and Gusevskaya, E. V. (2001). "Hydration and acetoxylation of monoterpenes catalyzed by heteropoly acid," *J. Mol. Catal. A- Chem*. 175(1-2), 33-42. DOI: 10.1016/S1381-1169(01)00217-5

Serrano-Ruiz, J. C., West, R. M., and Dumesic, J. A. (2010). "Catalytic conversion of renewable biomass resources to fuels and chemicals," *Annu. Rev. Chem. Biomol.* 1, 79-100. DOI: 10.1146/annurev-chembioeng-073009-100935

Shen, S., Wang, C., Cai, B., Li, H., Han, Y., Wang, T., and Qin, H. (2013). "Heterogeneous hydrolysis of cellulose into glucose over phenolic residue-derived solid acid," *Fuel* 113, 644-649. DOI: 10.1016/j.fuel.2013.06.021

Shu, Q., Gao, J., Nawaz, Z., Liao, Y., Wang, D., and Wang, J. (2010). "Synthesis of biodiesel from waste vegetable oil with large amounts of free fatty acids using a carbon-based solid acid catalyst," *Appl. Energ*. 87(8), 2589-2596. DOI: 10.1016/j.apenergy.2010.03.024

Song, D., An, S., Lu, B., Guo, Y., and Leng, J. (2015). "Arylsulfonic acid functionalized hollow mesoporous carbon spheres for efficient conversion of levulinic acid or furfuryl alcohol to ethyl levulinate," *Appl. Catal. B- Environ.* 179, 445–457. DOI: 10.1016/j.apcatb.2015.05.047

Song, X., Fu, X., Zhang, C., Huang, W., Zhu, Y., Yang, J., and Zhang, Y. (2012). "Preparation of a novel carbon based solid acid catalyst for biodiesel production *via* a sustainable route," *Catal. Lett.* 142(7), 869-874. DOI: 10.1007/s10562-012-0840-2

Tang, X., and Niu, S. (2019). "Preparation of carbon-based solid acid with large surface area to catalyze esterification for biodiesel production," *J. Ind. Eng. Chem*. 69, 187-195. DOI: 10.1016/j.jiec.2018.09.016

Tian, J., Liu, Z., Li, Z., Wang, W., and Zhang, H. (2017). "Hierarchical S-doped porous carbon derived from by-product lignin for high-performance supercapacitors," *RSC Adv*. 7(20), 12089-12097. DOI: 10.1039/c7ra00767a

Toda, M., Takagaki, A., Okamura, M., Kondo, J. N., Hayashi, S., Domen, K., and Hara, M. (2005). "Biodiesel made with sugar catalyst," *Nature* 438(7065), 178-178. DOI: 10.1038/438178a

Vital, J., Ramos, A. M., Silva, I. F., Valente, H., and Castanheiro, J. E. (2000). "Hydration of *α*-pinene over zeolites and activated carbons dispersed in polymeric membranes," *Catal. Today* 56(1-3), 167-172. DOI: 10.1016/S0920-5861(99)00273-4

Wang, J., Xing, S., Huang, Y., Fan, P., Fu, J., Yang, G., Yang, L., and Lv, P. (2017). "Highly stable gasified straw slag as a novel solid base catalyst for the effective synthesis of biodiesel: Characteristics and performance," *Appl. Energ*. 190, 703-712. DOI: 10.1016/j.apenergy.2017.01.004

Wang, J., Xu, W., Ren, J., Liu, X., Lu, G., and Wang, Y. (2011). "Efficient catalytic conversion of fructose into hydroxymethylfurfural by a novel carbon-based solid acid," *Green Chem*. 13(10), 2678-2681. DOI: 10.1039/c1gc15306d

Wang, L., Dong, X., Jiang, H., Li, G., and Zhang, M. (2014). "Preparation of a novel carbon-based solid acid from cassava stillage residue and its use for the esterification of free fatty acids in waste cooking oil," *Bioresource Technol*. 158, 392-395. DOI: 10.1016/j.biortech.2014.02.132

Yang, G., Liu, Y., Zhou, Z., and Zhang, Z. (2011). "Kinetic study of the direct hydration of turpentine," *Chem. Eng. J*. 168(1), 351-358. DOI: 10.1016/j.cej.2011.01.037

Yuan, B., Zhong, H., Liu, P., Liu, X., Xie, C., Yu, F., Yu, S., and Zhang, J. (2016). "Heteropolyacid bisalt of *n*-octyl ethoxylated octadecylamine: An efficient and reusable catalyst for carboxylic acid-free hydration of *α*-pinene," *Catal. Lett*. 146(5), 929-936. DOI: 10.1007/s10562-016-1709-6

Zeng, D., Liu, S., Gong, W., Wang, G., Qiu, J., and Chen, H. (2014). "Synthesis, characterization and acid catalysis of solid acid from peanut shell," *Appl. Catal. A-Gen.* 469, 284-289. DOI: 10.1016/j.apcata.2013.09.038

Zhang, L., He, Y., Zhu, Y., Liu, Y., and Wang, X. (2017). "*Camellia oleifera* shell as an alternative feedstock for furfural production using a high surface acidity solid acid catalyst," *Bioresource Technol*. 249, 536-541. DOI: 10.1016/j.biortech.2017.10.061

Zhao, J., Zhou, C., He, C., Dai, Y., Jia, X., and Yang, Y. (2016). "Efficient dehydration of fructose to 5-hydroxymethylfurfural over sulfonated carbon sphere solid acid catalysts," *Catal. Today* 264, 123-130. DOI: 10.1016/j.cattod.2015.07.005

Article submitted: January 19, 2019; Peer review completed: March 17, 2019; Revised version received: April 5, 2019; Accepted: April 6, 2019; Published: April 15, 2019.
DOI: 10.15376/biores.14.2.4284-4303